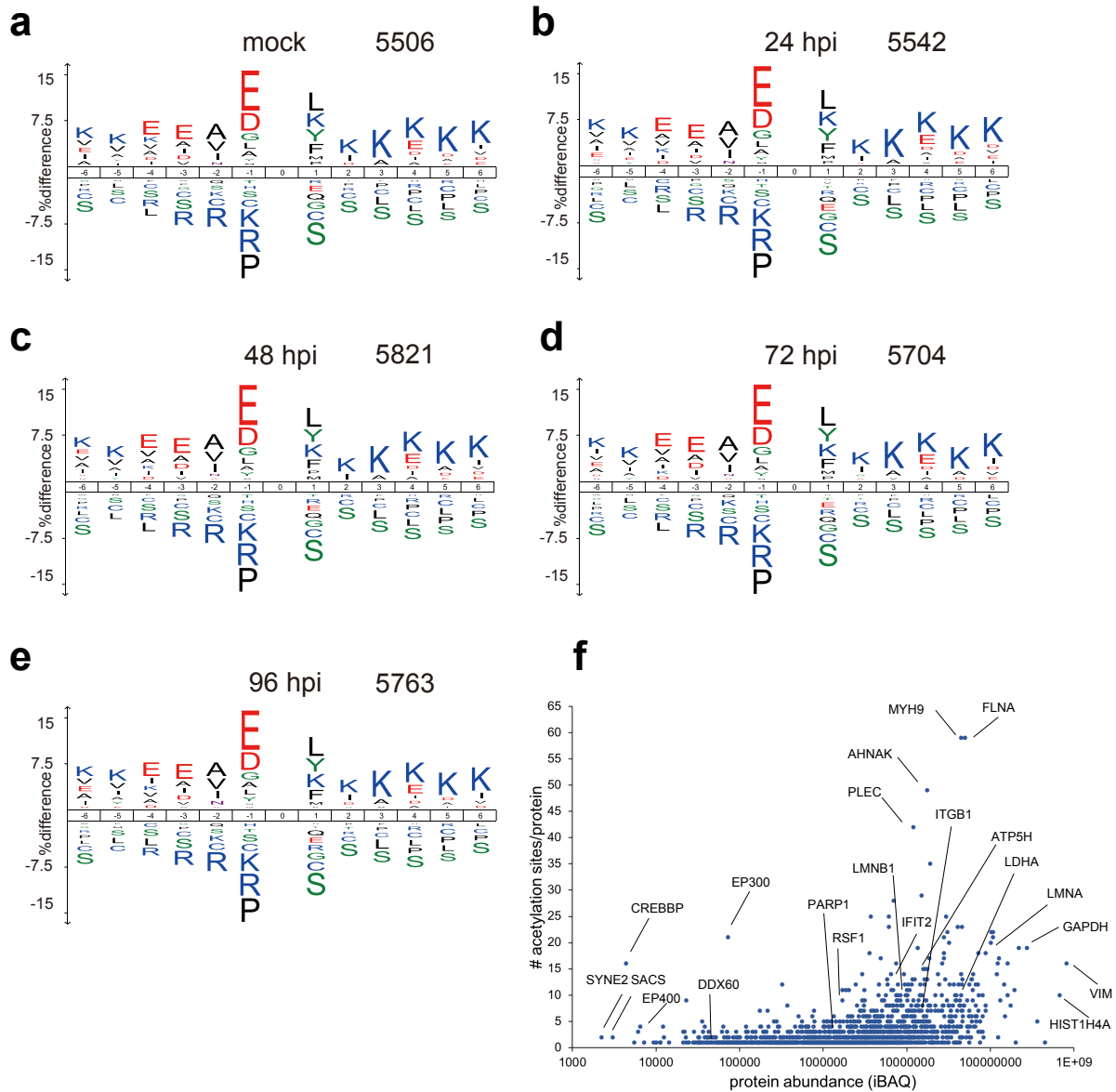


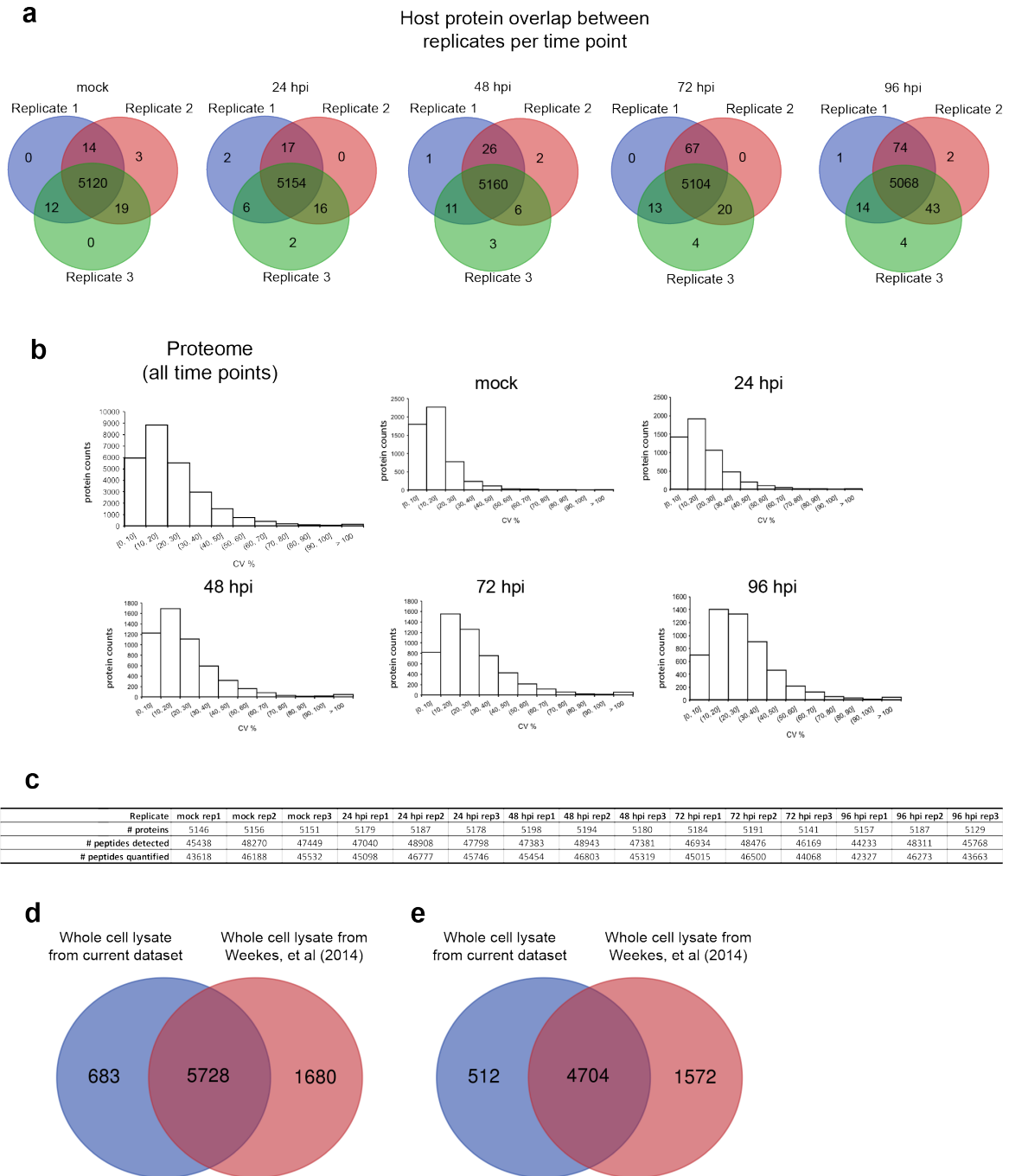
Orchestration of protein acetylation as a toggle for cellular defense and virus replication

Murray, et al.



Supplementary Figure 1. Analysis of acetylated cellular peptides from uninfected and infected cells. Motifs from **a** uninfected and infected cells at **b** 24 hpi, **c** 48 hpi, **d** 72 hpi, and **e** 96 hpi were analyzed by IceLogo. Data represent results from a percentage difference scoring method with a P-value cut-off equal to 0.01 for the six amino acids flanking the acetylated lysine. The height of the letter at each position represents the difference in the amino acid residue frequency between the experimental set and the reference set. Numbers on the top indicate the number of peptides used for generating IceLogos. **f** Relationship between number of acetylation

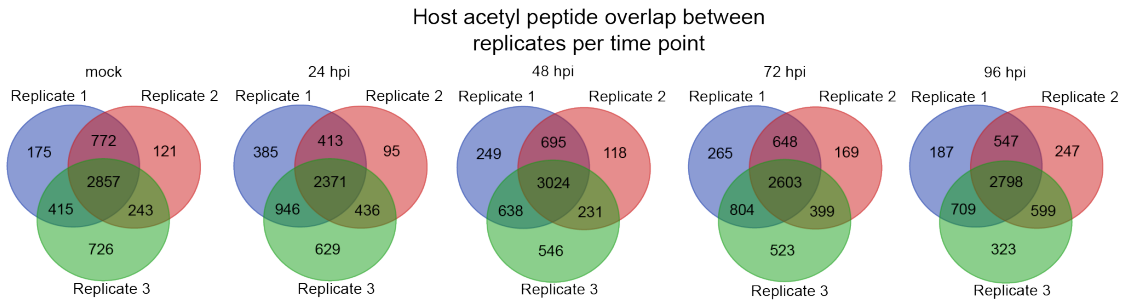
sites and corresponding protein abundance. Protein quantification was performed using the iBAQ algorithm.



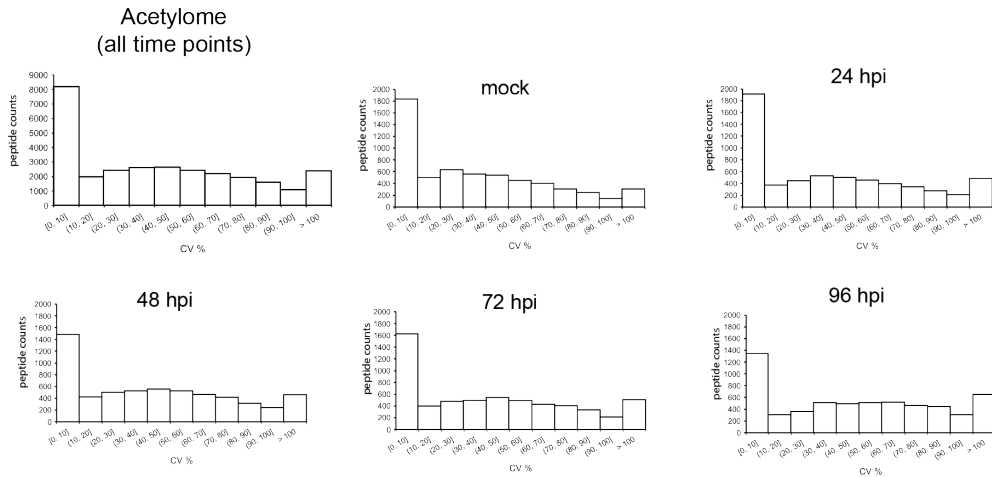
Supplementary Figure 2. Comparison of the proteome datasets from the biological replicates, as well as with prior literature. a Venn diagrams showing the overlap in host proteins quantified between three biological replicates at each time point during infection. **b** Distribution of the coefficient of variation (CV %) of all time points combined, and individual

time points for host whole proteome. **c** Comparison of number of host proteins and number of corresponding detected and quantified unmodified peptides across all three biological replicates in all time points. **d, e** Comparison of the number of identified proteins from the current proteome dataset and a previous study (Weekes, et al 2014). **d** Number of identified proteins with more one or more unique peptides (not including isoforms). **e** Number of identified proteins with two or more unique peptides (not including isoforms).

a



b

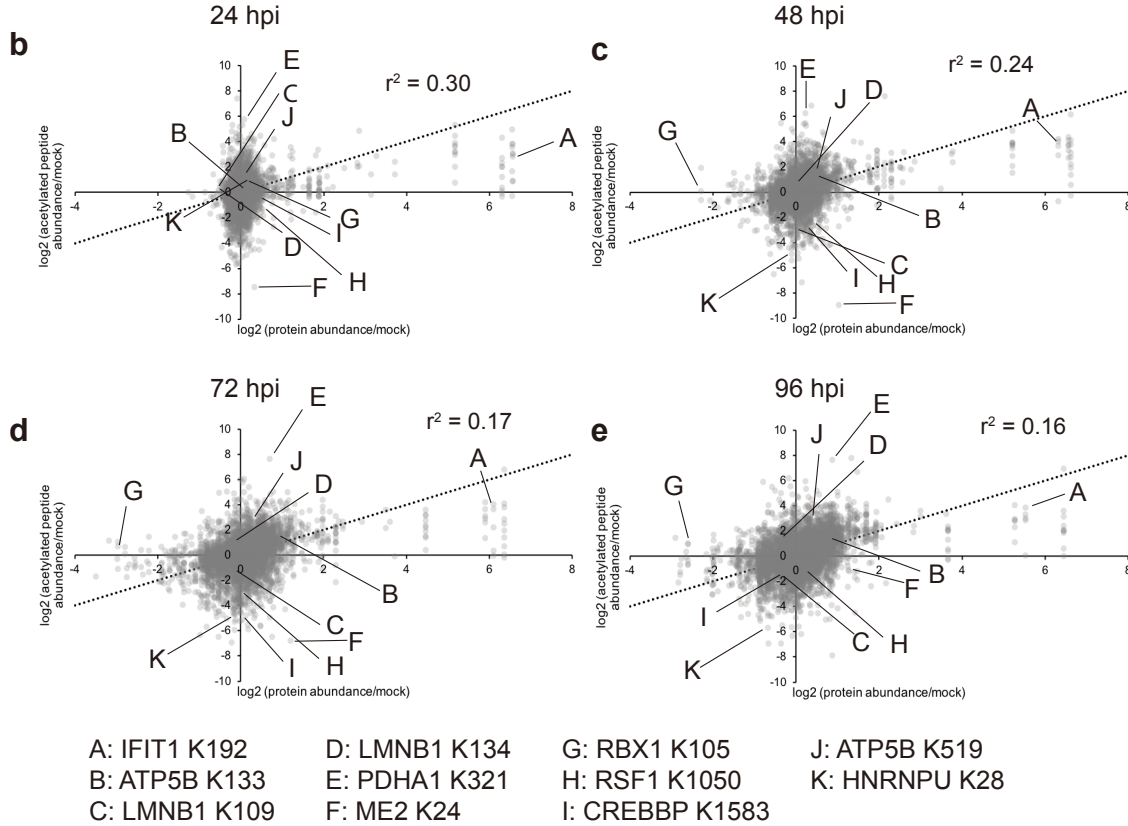


Supplementary Figure 3. Comparison of the acetylome datasets from the biological

replicates. a Venn diagrams showing the overlap in host acetylated peptides filtered and used in the quantification analysis between three biological replicates at each time point during infection. **b** Distribution of the coefficient of variation (CV %) of all time points combined, and individual time points for host peptides in the acetylome. CV percentages do not include imputed values.

a

Replicate	mock rep1	mock rep2	mock rep3	24 hpi rep1	24 hpi rep2	24 hpi rep3	48 hpi rep1	48 hpi rep2	48 hpi rep3	72 hpi rep1	72 hpi rep2	72 hpi rep3	96 hpi rep1	96 hpi rep2	96 hpi rep3
# acetylated peptides	4219	3993	4241	4115	3315	4382	4606	4068	4439	4320	3819	4329	4241	4191	4429
# acetylated proteins	1608	1563	1604	1606	1367	1631	1692	1559	1639	1610	1502	1593	1566	1590	1602
% imputed acetyl peptide abundance (only used for trend analysis)	27	31	26	29	42	24	20	29	23	25	34	25	26	27	23



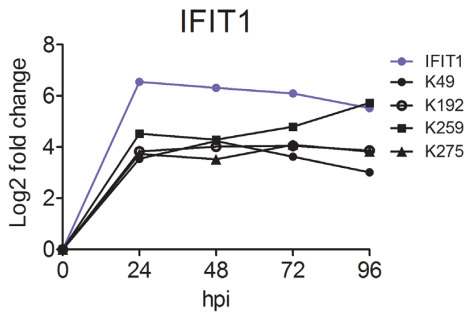
Supplementary Figure 4. Assessment of correlation between changes in acetylated peptide abundance and changes in protein abundance for host proteins. **a** Comparison of host acetylated peptides, the corresponding acetylated proteins, and the percentage of imputed values (used only in trend analyses in Figure 2b, Figure 3a, and Supplementary Figure 4b-e) across all three acetyl-IP biological replicates in all time points. These numbers represent the dataset of acetylated peptides that were filtered and used for quantitative analysis. **b-e** Dot plots of the log₂ fold change of acetylated peptide abundance (normalized to mock) and corresponding protein abundance (normalized to mock) at **b** 24, **c** 48, **d** 72, and **e** 96 hpi. Each dot represents one

acetylated peptide, and a number of peptides of interest are marked. The dotted line indicates a slope equal to 1.

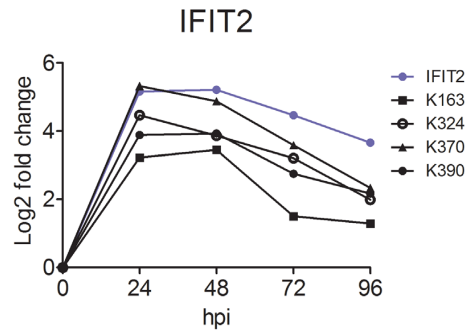
a

Cluster	# Proteins	Enriched GO Biological Processes	Representative Proteins	p-value	FDR
1	234	TCA cycle, response to virus, type I interferon signaling, gluconeogenesis	DLD, IFIT1, STAT1, GOT1	3.89E-14, 1.18E-05, 1.19E-05, 6.10E-05	5.11E-11, 1.74E-03, 1.74E-03, 4.45E-03
2	551	TCA cycle, glyoxylate metabolic process, tRNA aminoacylation for protein translation, canonical glycolysis, oxidative phosphorylation	PDHA, DLAT, MARS, ENO1, NDUFB6	2.22E-16, 8.40E-9, 5.11E-08, 1.03E-6, 1.82E-95	2.46E-13, 3.92E-06, 1.03E-05, 1.13E-04, 1.22E-03
3	641	translation, rRNA processing, cell-cell adhesion, TCA cycle, nucleosome assembly, glyoxylate metabolic process	RPL5, LDHA, ATP5O, SMARCA5, OGDH	1.11E-16, 1.11E-16, 1.11E-16, 4.28E-12, 1.19E-11, 5.57E-05	3.94E-14, 3.94E-14, 3.94E-14, 1.33E-09, 3.28E-09, 3.95E-03
4	833	translation, RNA processing, cell-cell adhesion, antigen processing and presentation, regulation of ubiquitin-protein ligase activity, NIK/NF-kappaB signaling, protein folding, viral process, canonical glycolysis, nucleosome assembly	RPL4, RUVBL1, MYO6, PSMD8, HSP90AB1, CREBBP, ENO1, KAT6B	1.11E-16, 1.11E-16, 1.11E-16, 1.11E-16, 1.11E-16, 5.77E-15, 2.93E-14, 2.49E-13, 9.94E-13, 6.69E-10, 1.27E-07, 5.85E-05	4.09E-14, 4.09E-14, 4.09E-14, 4.09E-14, 4.09E-14, 1.83E-12, 7.83E-12, 5.23E-11, 1.79E-10, 9.37E-08, 1.13E-05, 3.10E-03
5	662	translation, viral transcription, protein targeting to membrane, cell-cell adhesion, nucleosome assembly, mRNA splicing, histone H3 acetylation, protein stabilization	RPL4, FLNB, HIST2H2BF, HNRNPU, JADE1, HSP90AA1	1.11E-16, 1.11E-16, 1.11E-16, 1.11E-16, 2.67E-12, 1.59E-10, 8.56E-07, 5.24E-05	3.91E-14, 3.91E-14, 3.91E-14, 3.91E-14, 8.23E-10, 4.35E-08, 1.32E-04, 3.76E-03
6	329	cell-cell adhesion, translation, protein targeting to membrane, viral transcription, nucleosome assembly, rRNA processing, cell-junction assembly, regulation of mRNA stability	PFN1, EIF4A1, RPS9, H3F3A, ACTB, HNRNPD	2.19E-14, 2.13E-12, 2.82E-12, 7.14E-12, 3.00E-07, 4.77E-07, 6.45E-07, 2.52E-05	3.59E-11, 1.54E-09, 1.54E-09, 2.93E-09, 7.02E-05, 9.78E-05, 1.06E-04, 3.22E-03
7	230	beta-catenin-TCF complex assembly, nucleosome assembly	CREBBP, RSF1	7.34E-08, 6.81E-07	8.06E-05, 3.98E-04

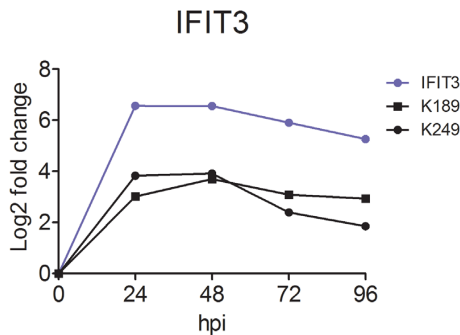
b



c



d

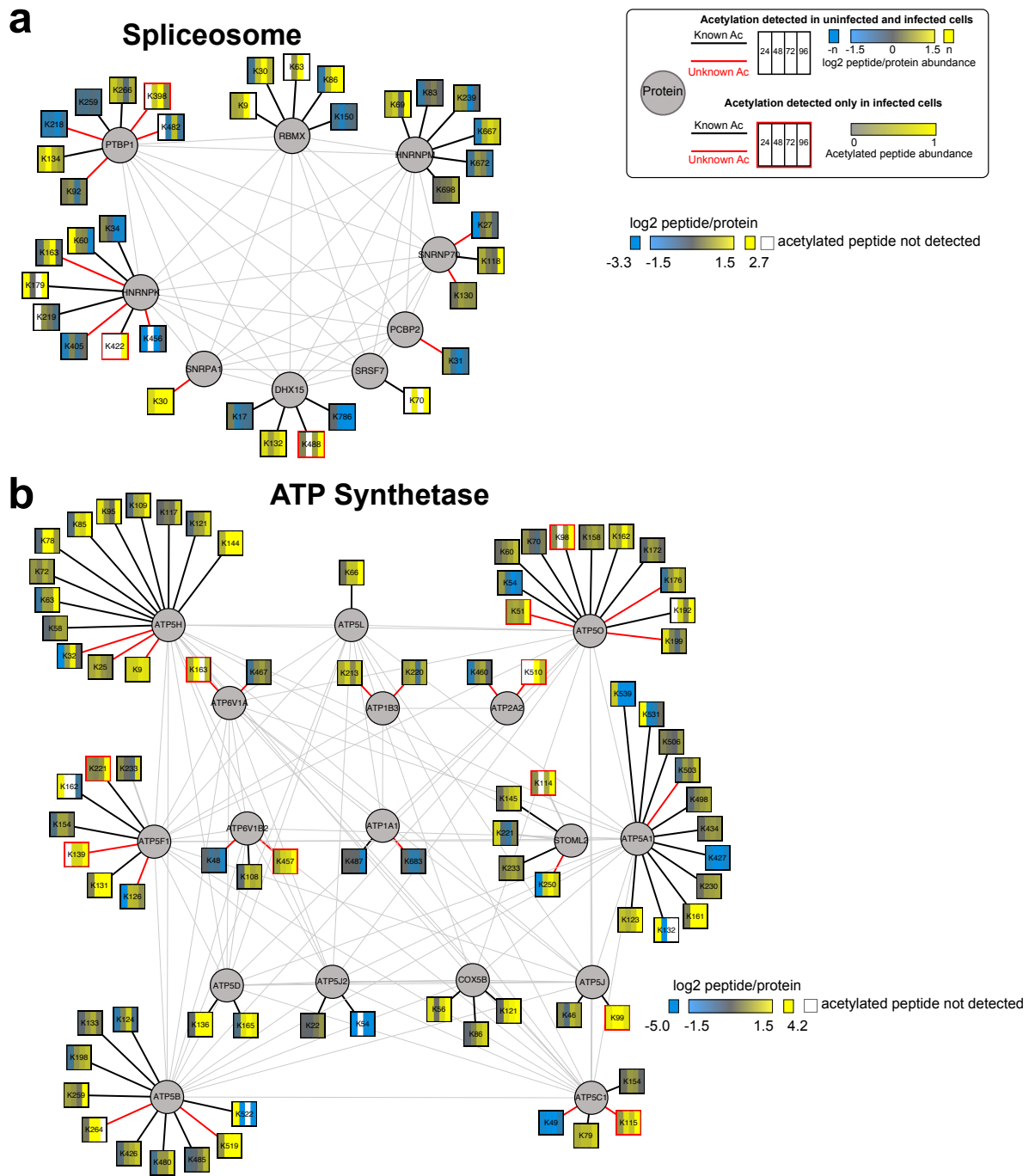


Supplementary Figure 5. Distinct acetylation abundance trends and different enriched GO

Biological Processes. a Enriched GO Biological Processes with p-values $\leq E-05$ were

determined for each acetyl trend cluster through the Reactome plugin in Cytoscape. The p-value

and FDR for each term are shown in the same order as the terms are shown. **b-e** Comparison of log₂ fold change of protein abundance to acetylated peptide abundance for IFIT proteins. IFIT protein abundance (normalized to mock) is shown in blue. Abundance of each acetylated peptide that was detected in both mock and infection time points is shown in black (normalized to mock). **b** IFIT1, **c** IFIT2, **d** IFIT3.

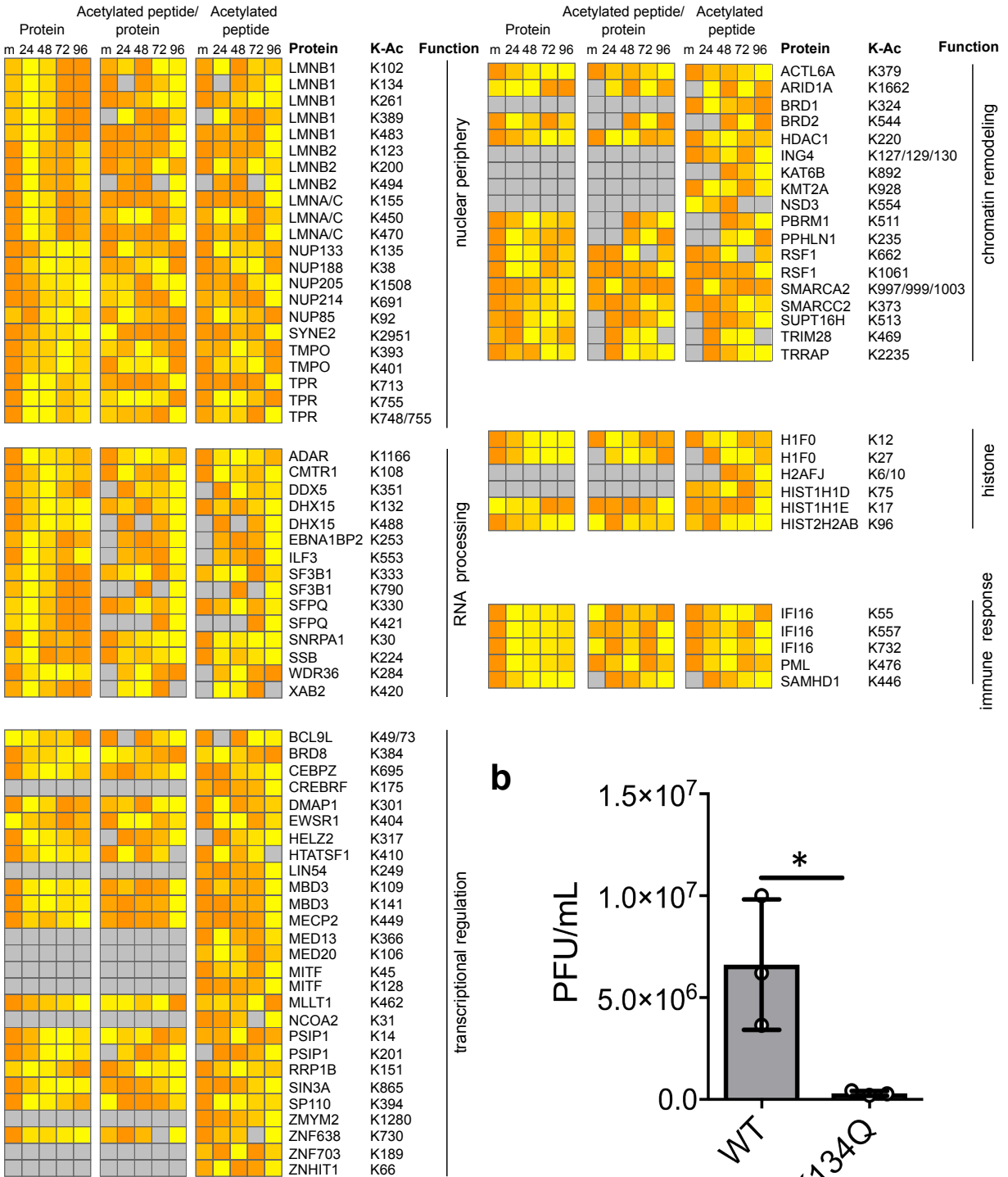
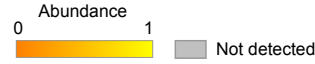


Supplementary Figure 6. Site-specific acetylation trends are observed on mRNA splicing and ATP synthetase proteins. a, b All detected acetylation sites on proteins from the indicated biological function representing different site-specific trends in acetylation during infection.

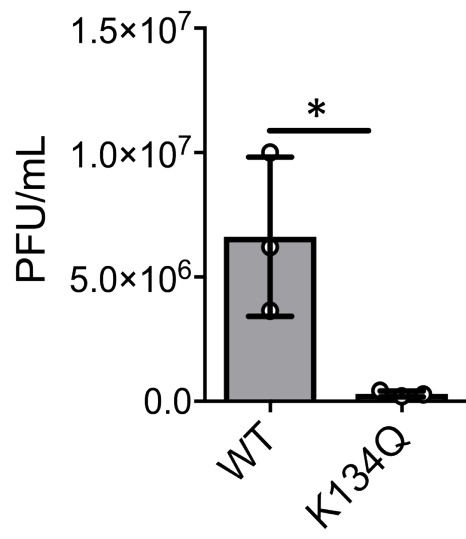
Log₂ peptide/protein values are shown unless the acetylated peptide was not identified in mock, in which case the acetylated peptide abundances during infection are shown scaled 0 to 1. **a** Spliceosome **b** ATP synthetase complex. Circles, proteins; squares, acetylation sites; red lines, previously unknown acetylation sites; black lines, known acetylation sites; black boxes, detected in mock; red boxes, only detected during infection. If a peptide was not quantified in a given time point, the corresponding column within the acetyl box is white.

a

Increasing acetylation in the nucleus



b



Supplementary Figure 7. Acetylation is increased on a subset of nuclear proteins, including those at the nuclear periphery such as LMNB1. **a** Sites on nuclear proteins with increased levels of acetylation during infection clustered by function. Abundances are scaled from 0 to 1 (left, protein abundance; middle, acetylated peptide abundance normalized to protein abundance; right, acetylated peptide abundance). **b** TCID₅₀ assessment of the effect of LMNB1 K134Q mutant on infectious extracellular virus produced. Average of three replicates ± SD. One-sided Student's t-test was used. * $p < 0.05$.

1. MATATPPP... 10 20 30 40 50 60 70 80 90 100 110 120 130 140
human
chimpanzee
gorilla
sumatran orangutan
olive baboon
green monkey
chusung macaque
mouse
rat
Western clawed frog
African clawed frog
zebrafish
turquoise killifish
bluefin notho

150
human
chimpanzee
gorilla
sumatran orangutan
olive baboon
green monkey
chusung macaque
mouse
rat
Western clawed frog
African clawed frog
zebrafish
turquoise killifish
bluefin notho

300
human
chimpanzee
gorilla
sumatran orangutan
green monkey
chusung macaque
zebrafish
turquoise killifish
bluefin notho

450
human
chimpanzee
gorilla
sumatran orangutan
green monkey
chusung macaque
mouse
bovine
Western clawed frog
African clawed frog
zebrafish
turquoise killifish
bluefin notho

500
human
chimpanzee
gorilla
sumatran orangutan
green monkey
chusung macaque
mouse
bovine
Western clawed frog
African clawed frog
zebrafish
turquoise killifish
bluefin notho

550
human
chimpanzee
gorilla
sumatran orangutan
green monkey
chusung macaque
mouse
bovine
Western clawed frog
African clawed frog
zebrafish
turquoise killifish
bluefin notho

600
human
chimpanzee
gorilla
sumatran orangutan
green monkey
chusung macaque
mouse
bovine
Western clawed frog
African clawed frog
zebrafish
turquoise killifish
bluefin notho

650
human
chimpanzee
gorilla
sumatran orangutan
green monkey
chusung macaque
mouse
bovine
Western clawed frog
African clawed frog
zebrafish
turquoise killifish
bluefin notho

700
human
chimpanzee
gorilla
sumatran orangutan
green monkey
chusung macaque
mouse
bovine
Western clawed frog
African clawed frog
zebrafish
turquoise killifish
bluefin notho

750
human
chimpanzee
gorilla
sumatran orangutan
green monkey
chusung macaque
mouse
bovine
Western clawed frog
African clawed frog
zebrafish
turquoise killifish
bluefin notho

800
human
chimpanzee
gorilla
sumatran orangutan
green monkey
chusung macaque
mouse
bovine
Western clawed frog
African clawed frog
zebrafish
turquoise killifish
bluefin notho

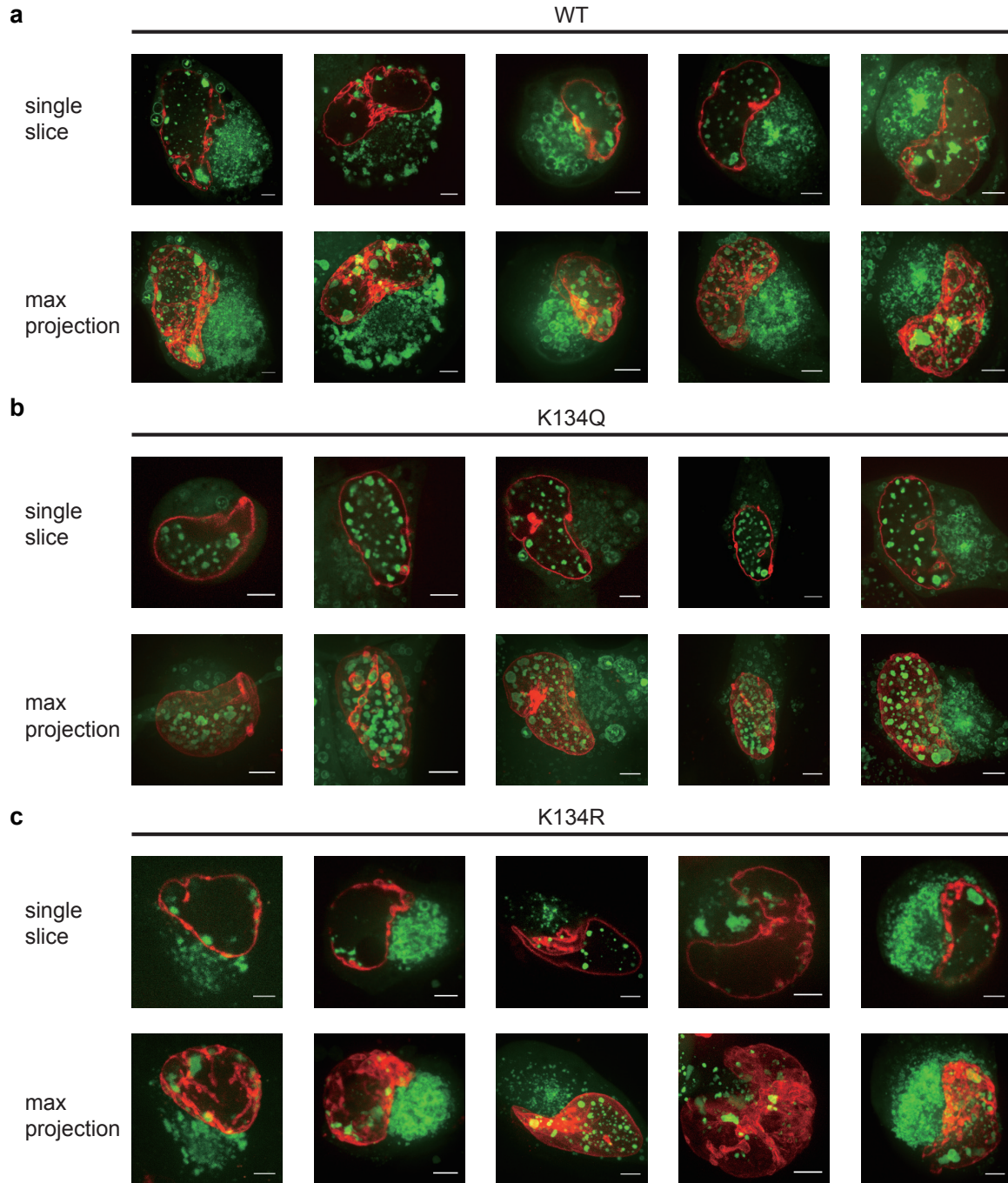
850
human
chimpanzee
gorilla
sumatran orangutan
green monkey
chusung macaque
mouse
bovine
Western clawed frog
African clawed frog
zebrafish
turquoise killifish
bluefin notho

900
human
chimpanzee
gorilla
sumatran orangutan
green monkey
chusung macaque
mouse
bovine
Western clawed frog
African clawed frog
zebrafish
turquoise killifish
bluefin notho

950
human
chimpanzee
gorilla
sumatran orangutan
green monkey
chusung macaque
mouse
bovine
Western clawed frog
African clawed frog
zebrafish
turquoise killifish
bluefin notho

1000
human
chimpanzee
gorilla
sumatran orangutan
green monkey
chusung macaque
mouse
bovine
Western clawed frog
African clawed frog
zebrafish
turquoise killifish
bluefin notho

Supplementary Figure 8. Sequence alignment of identified LMNB1 acetylated lysines and regulatory phosphorylated serines from different vertebrate species. Protein amino acid sequences from 16 species were retrieved from Uniprot, aligned by MultAlin, and colored by ESPript3. The conserved acetylated lysine sites detected in this study are highlighted in yellow and conserved phosphorylated serine sites of known function are highlighted in cyan.

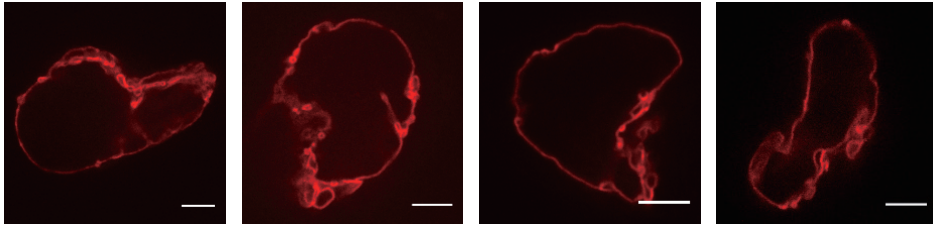


Supplementary Figure 9. Acetylation of LMNB1 impedes nuclear capsid egress. Additional examples of live cell confocal fluorescence microscopy images of cells transfected with **a** mCherry-LMNB1 WT, **b** K134Q, or **c** K134R (red) and infected with HCMV AD169 UL32-

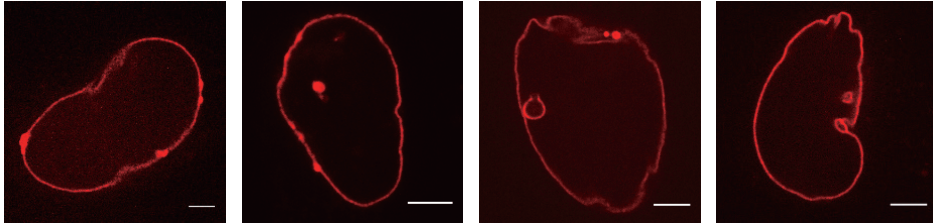
GFP (green) at 120 hpi. Five representative images for each construct are shown as a single slice through the center of the Z-stack (upper row) and as a maximum projection of the Z-stack (bottom row). The rightmost images for each construct are the single slice and maximum projection that correspond to the images shown in Figure 5a; scale bar = 5 μ m.

96 hpi

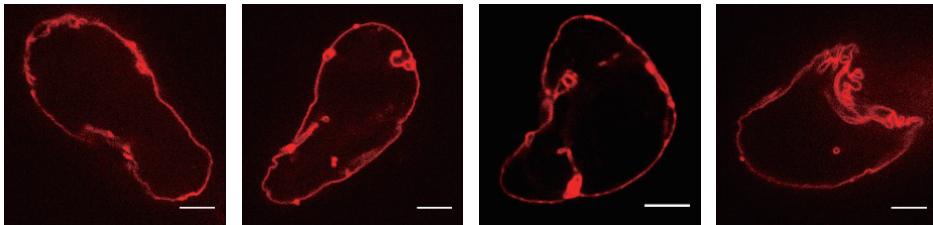
WT



K134Q

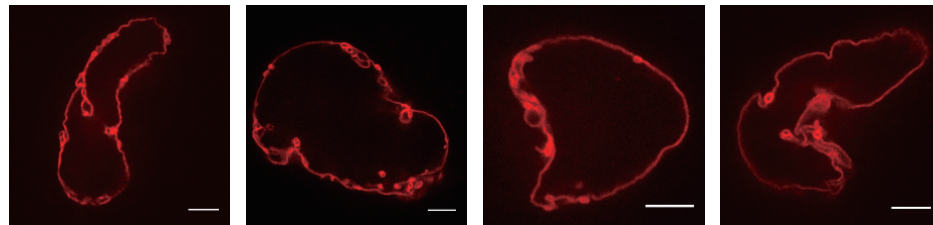


K134R

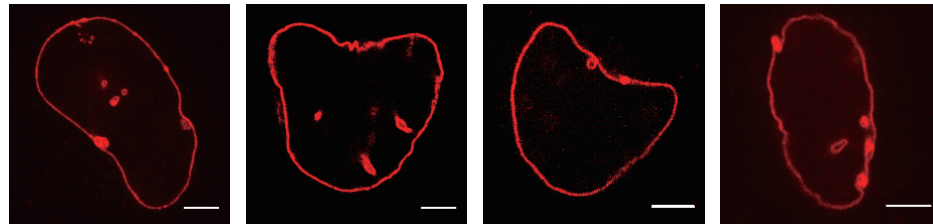


120 hpi

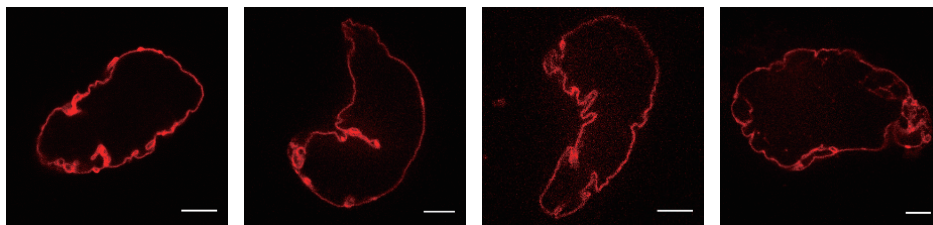
WT



K134Q



K134R



Supplementary Figure 10. Acetylation at K134 on LMNB1 decreases nuclear periphery disruption. Cells transfected with mCherry-LMNB1 WT, K134Q, or K134R (red) and infected with HCMV were imaged by live cell confocal fluorescence microscopy at 96 and 120 hpi. Four representative images for each LMNB1 construct per time point are shown as a single slice through the center of the Z-stack; scale bar = 5 μ m.

a

Replicate	24 hpi rep1	24 hpi rep2	24 hpi rep3	48 hpi rep1	48 hpi rep2	48 hpi rep3	72 hpi rep1	72 hpi rep2	72 hpi rep3	96 hpi rep1	96 hpi rep2	96 hpi rep3
# acetylated peptides	17	10	19	15	13	27	18	13	29	24	16	31
# acetylated proteins	12	8	13	11	9	17	13	9	19	14	11	19

b

Replicate	24 hpi rep1	24 hpi rep2	24 hpi rep3	48 hpi rep1	48 hpi rep2	48 hpi rep3	72 hpi rep1	72 hpi rep2	72 hpi rep3	96 hpi rep1	96 hpi rep2	96 hpi rep3
# proteins	75	73	77	79	79	88	83	85	90	89	90	91
# peptides detected	376	380	482	527	528	791	680	766	944	787	917	1007
# peptides quantified	349	354	406	504	504	584	660	739	767	761	885	912

c

Capsid					
Protein	Domain region (aa)	Domain region function	Protein length (aa)	Temporal expression	Acetylated lysine(s)
UL46			290	L	25, 270
UL85			306	L	15, 23, 166
UL86	1-59 60-189, 234-290, 363-397, 1032-1106 190-233 291-362 388-480, 1322-1370 481-1031 1107-1321	N-lasso Johnson fold helix-hairpin dimerization channel upper region buttress	1370	L	24, 85, 116, 165, 220, 377, 413, 415, 439, 513, 1257, 1280, 1336
Envelope					
Protein	Domain region (aa)	Domain region function	Protein length (aa)	Temporal expression	Acetylated lysine(s)
gB	1-31 92-111 152-158 237-244 411-447 686-748 694-897	signal peptide disintegrin-like domain involved in fusion and/or binding to host membrane involved in fusion and/or binding to host membrane required to assemble an antigenic region hydrophobic membrane proximal region internalization motif	906	DE	230, 370, 633, 669, 699
gM (UL100)	1-13 14-34 35-79 80-100 101-126 127-147 148-151 152-172 173-200 201-221 222-239 240-260 261-264 265-285 286-298 299-319 320-372 300-372 1-118	intravirion helical virion surface intravirion helical virion surface helical intravirion helical virion surface helical intravirion helical virion surface helical intravirion helical intravirion interacts with FIP4 region that binds gN	372	L	8, 108, 331
gL	1-30	signal peptide	278	L	248
gH (UL75)	24-270 218-281 721-741 742-743	virion surface interacts with gL helical intravirion	743	L	131, 327, 405
gO (UL74)	80-100	helical	466	L	188
IRL10	24-294 295-317 318-345	virion surface helical intravirion	345	DE	175

Tegument					
Protein	Domain region (aa)	Domain region function	Protein length (aa)	Temporal expression	Acetylated lysine(s)
UL25			666	L	609
UL26	1-34 184-222	important for viral growth essential for replication	222	DE	203
UL32	1-275 982-1048	capsid (SCP) binding region C terminal interacts with UL96	1048	DE	237, 373, 384, 805, 903, 1000
UL35			640	DE	118
UL43			423	L	135
UL44	1-309 1-290 162-174 425-431 40-433 291-433 129-140 1-290	needed for function as a processivity factor self-dimerization highly flexible loop, involved in DNA binding NLS interacts with UL112/113 interacts with UL114 connector loop, interacts with UL64 interacts with UL84	433	DE	101, 288, 338, 376
UL45	1-200, 313, 433	interacts with Ubc9	906	DE	523, 614
UL47	474-983	interaction with UL48	983	L	281
UL48	1-238 322-754	deubiquitination activity interacts with UL47	2241	DE	439, 465, 481, 595, 640, 800, 1001, 1003, 1019, 1175, 1261, 1288, 1478
UL50	52-80, 125 139 1-169	heterodimerization with UL53 conserved	397	DE	20, 132
UL54	379-421 492-588 696-742 771-790 805-845 905-919 962-970 978-988 1153-1159 1222-1227 1220-1249 1-1212	conserved with other DNA-dependent DNA polymerases (labeled in an order): IV, 5- region C, II, VI, III, I, VII, VI, I, II, III, binding of deoxynucleoside triphosphates, chelating the Mg ²⁺ ion, and interacting with primer and template; IV and 5-region C: 3' to 5' exonuclease function NLSA NLSB interaction with UL44 interaction with UL114	1242	DE	500
UL69	17-30 35-46, 122, 132 387-501 596-624	UAP56 interaction RNA binding domain zinc finger CHC2-type NES	744	L	275, 580
UL82			599	L	91, 376
UL83	1-386 387-470 471-561	pyrin association domain linker conserved C terminal domain and NLS	561	L	154, 176, 181, 215, 283, 378, 509, 538, 557
UL84	1-68 101-200 161-170 229-238 360-367	association with pUL44 and viral DNA replication interaction with CK2, essential for DNA replication nuclear localization signal nuclear export signal 1 nuclear export signal 2	587	DE	94, 339, 436
UL94			345	DE	306, 316, 324
UL96	1-101 122-127	interaction with UL32 critical for virus maturation	127	DE	10
UL97	48-110 292-707 337-345 352-380 373-381 433-450	NLS important for phosphorylation activity ATP binding/ Domain I (sim to PK) Domain II (sim to PK) Domain III (sim to PK) Domain V (sim to PK)	707	DE	586
UL122	200-208	non-covalent SUMO1 binding region	580	IE	21, 161, 337, 421
US22			576	DE	197, 305, 358

Supplementary Figure 11. Viral acetylome. **a** Comparison of the number of viral acetylated peptides and the corresponding acetylated viral proteins across all three acetyl-IP biological replicates in all infection time points. **b** Comparison of the number of viral proteins and the number of corresponding detected and quantified unmodified peptides across all three biological

replicates in all infection time points from the whole proteome dataset. **c** Functional domains, temporal expression, and acetylated lysine sites detected in this study on HCMV proteins known to be part of the capsid, envelope, and tegument. All domain information is annotated from Uniprot and primary literature.